Structures of Reactive Nitrenium Ions: Time-Resolved Infrared Laser Flash Photolysis and Computational Studies of Substituted *N*-Methyl-*N*-arylnitrenium Ions

Sanjay Srivastava,[†] Patrick H. Ruane,[†] John P. Toscano,*,[†] Michael B. Sullivan,[‡] Christopher J. Cramer,*,[‡] Dominic Chiapperino,[§] Elizabeth C. Reed,[§] and Daniel E. Falvey*,[§]

Contribution from the Department of Chemistry, Johns Hopkins University, 3400 North Charles Street, Baltimore, Maryland 21218-2685, Department of Chemistry and Supercomputer Institute, University of Minnesota, 207 Pleasant Street SE, Minneapolis, Minnesota 55455-0431, and Department of Chemistry and Biochemistry, University of Maryland, College Park, Maryland 20742-2021

Abstract: A series of para-substituted *N*-methyl-*N*-phenylnitrenium ions (*N*-(4-biphenylyl)-*N*-methylnitrenium ion, *N*-(4-chlorophenyl)-*N*-methylnitrenium ion, *N*-(4-methoxyphenyl)-*N*-methylnitrenium ion, and *N*-(4-methylphenyl)-*N*-methylnitrenium ion) were generated through photolysis of the appropriately substituted 1-aminopyridinium salt. Laser flash photolysis using UV−vis detection as well as photoproduct analysis verified that the expected nitrenium ions were formed cleanly and rapidly following photolysis. Laser flash photolysis with time-resolved infrared detection allowed for structural characterization of the nitrenium ions through observation of a symmetrical aromatic C═C stretch in the region 1580−1628 cm^{-1}. The specific frequencies reflect the degree of quinoidal character present in each phenylnitrenium ion (i.e., the degree to which the nitrenium ion resembles a 4-iminocyclohexa-2,5-dienyl cation). The 4-methoxy derivative shows the highest frequency C═C stretch, indicating that this strongly π-electron-donating substituent imparts more quinoidal character, and the 4-chloro derivative shows the lowest frequency C═C stretch, suggesting that it possesses the least quinoidal character. Quantum calculations using density functional theory (BPW91/cc-pVDZ) were carried out on the same nitrenium ions. The theoretically derived IR frequencies showed excellent quantitative agreement with the experiment. The computed structures show significant bond length alternation in the phenyl rings, shortened C−N bond lengths, and substantial positive charge delocalization into the phenyl rings. All of these effects are more pronounced with increasing π-donating character of the ring substituent. Arylnitrenium ions are well described as 4-iminocyclohexa-2,5-dienyl cations.

Introduction

Arylnitrenium ions are short-lived, electrophilic species,[1−4] which have received considerable attention in recent years due to their suspected role in chemical carcinogenesis.[5−8] It is known that certain aromatic amines, such as 2-acetylaminofluorene, are enzymatically converted into sulfate esters of the corresponding *N*-hydroxylamines. It is now clear that in aqueous media such esters spontaneously eliminate a sulfate anion, producing an arylnitrenium ion.[9,10] It has further been demonstrated that appropriately substituted arylnitrenium ions can be selectively trapped by guanine bases in DNA.[2,6,8,11−13] This trapping event is thought to lead to carcinogenic mutations.[14]

Despite this biochemical interest there is very little detailed experimental information on arylnitrenium ion structures. The inherent instability of these species usually renders them unsuitable for X-ray crystallography or high-resolution NMR. (However, certain highly stabilized nitrenium ions have been examined with these techniques.[15]) Most of the knowledge regarding reactive arylnitrenium ion structures comes from quantum chemical calculations.[16−23] Phenylnitrenium ion (PhNH$^+$) is the simplest example of the arylnitrenium ions and has thus

---

[†] Johns Hopkins University.

[‡] University of Minnesota.

[§] University of Maryland.

(1) Simonova, T. P.; Nefedov, V. D.; Toropova, M. A.; Kirillov, N. F. *Russ. Chem. Rev.* **1992**, *61*, 584−599.

(2) McClelland, R. A.; Gadosy, T. A.; Ren, D. *Can. J. Chem.* **1998**, *76*, 1327−1337.

(3) McClelland, R. A. *Tetrahedron* **1996**, *52*, 6823−6858.

(4) Abramovitch, R. A.; Jeyaraman, R. In *Nitrenium Ions*; Scriven, E. F. V., Ed.; Academic: Orlando, FL, 1984; pp 297−357.

(5) Kadlubar, F. F. In *DNA Adducts of Carcinogenic Amines*; Hemminki, K., Dipple, A., Shuker, D. E. G., Kadlubar, F. F., Segerbäck, D. and Bartsch, H., Ed.; Oxford University Press: Oxford, UK, 1994; pp 199−216.

(6) Humphreys, W. G.; Kadlubar, F. F.; Guengerich, F. P. *Proc. Natl. Acad. Sci. U.S.A.* **1992**, *89*, 8278−8282.

(7) Novak, M.; Kennedy, S. A. *J. Phys. Org. Chem.* **1998**, *11*, 71−76.

(8) McClelland, R. A.; Ahmad, A.; Dicks, A. P.; Licence, V. *J. Am. Chem. Soc.* **1999**, *121*, 3303−3310.

(9) Novak, M.; Kahley, M. J.; Lin, J.; Kennedy, S. A.; James, T. G. *J. Org. Chem.* **1995**, *60*, 8294−8304.

(10) Novak, M.; VandeWater, A. J.; Brown, A. J.; Sanzebacher, S. A.; Hunt, L. A.; Kolb, B. A.; Brooks, M. E. *J. Org. Chem.* **1999**, *64*, 6023−6031.

(11) Novak, M.; Kennedy, S. A. *J. Am. Chem. Soc.* **1995**, *117*, 574−575.

(12) Meier, C.; Boche, G. *Tetrahedron Lett.* **1990**, *31*, 1693−1696.

(13) Famulok, M.; Boche, G. (University of Marburg, Germany). *Angew. Chem., Int. Ed. Engl.* **1989**, *28*, 468−469.

(14) Hoffman, G. R.; Fuchs, R. P. P. *Chem. Res. Toxicol.* **1997**, *10*, 347−359.

(15) Boche, G.; Andrews, P.; Harms, K.; Marsch, M.; Rangappa, K. S.; Schimeczek, M.; Willecke, C. *J. Am. Chem. Soc.* **1996**, *118*, 4925−4930.

Scheme 1. Nitrenium Ion Structure and Behavior

Chart 1. Nitrenium Ions
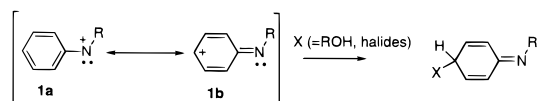
been the focus of several theoretical investigations. A recent computational study of phenylnitrenium ion using density functional theory (DFT) predicts this species to be a planar singlet in its ground state with the lowest energy triplet state 21.2 kcal/mol higher in energy.[16] An analysis of the computed geometry reveals the singlet to possess a shortened C−N bond and significant bond alternation in the phenyl ring. This result, together with the predicted charge distribution, suggests that the structure of PhNH$^+$ resembles the 4-iminocyclohexa-2,5-dienyl structure **1b** more closely than structure **1a**, where the positive charge is localized on N (Scheme 1). The latter is consistent with the observation that aromatic nitrenium ions react with nucleophiles (e.g., N$_3^-$, Cl$^-$, H$_2$O) on the aromatic ring rather than on nitrogen[24−26] (although for reasons that remain obscure, guanine, glutathione, and some aromatic amines are observed to react at nitrogen).

Experimentally, it is possible to directly detect reactive arylnitrenium ions using laser flash photolysis (LFP) and related photochemical methods. In its traditional implementation, the LFP experiment provides a time-resolved UV−visible absorption spectrum of the transient species of interest (LFP-TRUV). From this it is possible to obtain accurate lifetimes for the intermediate and rate constants for its reactions with added traps. A number of substituted arylnitrenium ions have been characterized in this manner, although the parent system, PhNH$^+$ remains elusive. Generally speaking, arylnitrenium ions are observed to react with anionic nucleophiles (N$_3^-$, Cl$^-$, etc.) at or near the diffusion limit. Neutral nucleophiles such as alcohols and water react several orders of magnitude more slowly, with rate constants that are sensitive to substitution on the ring of the arylnitrenium ion.[3,26−29]

One of the problems that has plagued studies of nitrenium ions, and indeed all short-lived intermediates, is finding meaningful ways of comparing theoretical calculations with experiments. The sorts of data readily available from experiments (UV−vis absorption spectra, reaction rate constants, stable product distributions) are notoriously difficult and/or expensive to compute to the requisite accuracy. Likewise, the parameters

that can be conveniently calculated from quantum mechanics (singlet−triplet state energy gaps, equilibrium geometries, etc.) are extremely difficult to determine experimentally, especially for transient molecules in solution.

Recently, several of us have communicated results from time-resolved infrared laser flash photolysis (LFP-TRIR) studies on diphenylnitrenium ion.[30] The LFP-TRIR experiment is conceptually similar to LFP-TRUV in that the transient intermediates are generated using a short pulse of laser light. The TRIR experiment, however, uses IR absorption rather than UV−vis to detect the transient species. Thus, it is possible to detect key IR bands for the transient species and compare them to spectra derived from quantum calculations. Unlike the situation with UV−vis spectra, it is a relatively simple matter to compute IR spectra for ground-state molecules. In the case of Ph$_2$N$^+$ the TRIR experiment revealed several bands. The band at 1392 cm^{-1} is assigned to a composite C−N=C stretch on the basis of isotope substitution experiments. Detected in the same experiment was a band at 1568 cm^{-1} due to an aromatic ring stretching.

Herein we describe experimental TRIR and TRUV studies on a series of substituted methylarylnitrenium ions (**2−5**, Chart 1). These measurements are compared with spectra for the singlet states calculated using state-of-the-art DFT methods. Excellent quantitative agreement between theoretically calculated and experimentally measured IR spectra is obtained. This study yields three major conclusions regarding the nitrenium ions. First, the observation of the characteristic IR bands in the TRIR, coupled with the isolation of nitrenium ion products, removes any doubt that arylnitrenium ions are the direct products from photolysis of the 1-aminopyridinium ions. Second, the calculated IR spectra for the singlet state nitrenium ions show a much better match with the experimental IR spectra than the calculated spectra for the corresponding triplet-state nitrenium ions. This confirms the long-held belief that simple aromatic nitrenium ions **2−5** are ground-state singlets, rather than triplets. Finally, analysis of the stretching frequencies and the theoretically derived bond lengths shows that the arylnitrenium ions all possess considerable quinoidal character (i.e., their structures are closer to **1b** than **1a**). This tendency is enhanced with π-donating substitutents.

Results

1. Synthesis of Photochemical Precursors to the Nitrenium Ions. The *N*-methyl-*N*-arylnitrenium ions (**2−5**) are generated through photolysis of appropriate 1-aminopyridinium salt derivatives.[31] The latter can be prepared using the synthetic route in Scheme 2. The appropriate *N*-methylaniline derivative (**7−10**) is first nitrosated with HCl/NaNO$_2$ to give *N*-nitrosoaniline derivatives (**11−14**) and then reduced with Zn, providing the 1,1-disubstituted hydrazine derivative (e.g., **19**). This was then condensed with 2,4,6-trimethylpyrylium tetrafluoroborate (**20**), providing the BF$_4^-$ salts of **15−18**. The latter can be isolated as crystalline solids and were characterized by the customary spectroscopic methods. In the case of **15** the hydrazine derivative **19** was isolated and characterized. For the

(16) Cramer, C. J.; Dulles, F. J.; Falvey, D. E. *J. Am. Chem. Soc.* **1994**, *116*, 9787−9788.

(17) Novak, M.; Lin, J. *J. Org. Chem.* **1999**, *64*, 6032−6040.

(18) Cramer, C. J.; Falvey, D. E. *Tetrahedron Lett.* **1997**, *38*, 1515−1518.

(19) Falvey, D. E.; Cramer, C. J. *Tetrahedron Lett.* **1992**, *33*, 1705−1708.

(20) Ford, G. P.; Herman, P. S. *J. Am. Chem. Soc.* **1989**, *111*, 3987−3996.

(21) Ford, G. P.; Herman, P. S.; Thompson, J. W. *J. Comput. Chem.* **1999**, *20*, 231−243.

(22) Li, Y.; Abramovitch, R. A.; Houk, K. N. *J. Org. Chem.* **1989**, *54*, 2911−2914.

(23) Sullivan, M. B.; Brown, K.; Cramer, C. J.; Truhlar, D. G. *J. Am. Chem. Soc.* **1998**, *120*, 11778−11783.

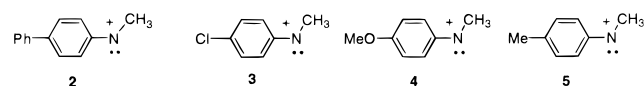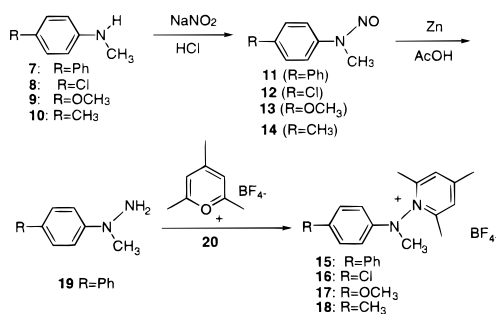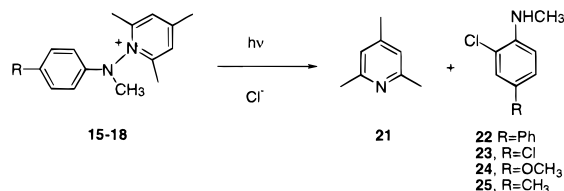(24) Gassman, P. G.; Campbell, G. A. *J. Am. Chem. Soc.* **1971**, *93*, 2567−2569.

(25) Gassman, P. G.; Campbell, G. A.; Frederick, R. C. *J. Am. Chem. Soc.* **1972**, *94*, 3884−3891.

(26) Ren, D.; McClelland, R. A. *Can. J. Chem.* **1998**, *76*, 78−84.

(27) Robbins, R. J.; Yang, L. L.-N.; Anderson, G. B.; Falvey, D. E. *J. Am. Chem. Soc.* **1995**, *117*, 6544−6552.

(28) Sukhai, P.; McClelland, R. A. *J. Chem. Soc., Perkin Trans. 2* **1996**, 1529−1530.

(29) Robbins, R. J.; Laman, D. M.; Falvey, D. E. *J. Am. Chem. Soc.* **1996**, *118*, 8127−8135.

(30) Srivastava, S.; Toscano, J. P.; Moran, R. J.; Falvey, D. E. *J. Am. Chem. Soc.* **1997**, *119*, 11552−11553.

(31) Balaban, A. T. *Tetrahedron* **1968**, *24*, 5059−5065.

Structures of Reactive Nitrenium Ions

J. Am. Chem. Soc., Vol. 122, No. 34, 2000 8273

Scheme 2. Precursor Synthesis

Figure 1. Transient UV−vis absorption spectra generated from LFP (308 nm, 10 ns 20 mJ/pulse) of **11** in CH₃CN taken 2, 5, 10, 20, and 40 μs after the laser pulse.

Scheme 3. Photolysis of Precursors and Stable Products

Scheme 4. Mechanism of Chloride Addition

other members of this series, it proved more efficient to trap the corresponding hydrazine derivatives in situ by adding an appropriate amount of the pyrylium salt to the reaction mixture.

2. Stable Photoproducts. The photolysis of 1-aminopyridinium salts has been shown to produce nitrenium ions through heterolytic scission of the N−N bond. This has previously been demonstrated for some 1-(*N,N*-diarylamino)pyridinium ions,[32] the 1-aminopyridinum ions,[33,34] and several other related systems.[35−40] The precursors used in this study show photochemical behavior consistent with this generalization. Each decomposes rapidly when irradiated with UV light to produce 2,4,6-trimethylpyridine **21** (Scheme 3). This product was observed by both GC/MS and ¹H NMR of the photolysis mixtures. Formation of this product verifies that the anticipated N−N bond scission occurs.

In addition to **21**, products characteristic of nitrenium ions were also detected by GC/MS. Specifically, photolysis of **15**−**18** in the presence of ca. 5−20 mM chloride ion gives chloride adducts **22**−**25**. (Scheme 3) These result from addition of Cl⁻ at the ring position *ortho* to the nitrenium ion center. Nucleophiles such as chloride are also known to add *para* to the nitrenium ion center.[25,41] However, when there is a substituent in this position, we assume that the initial *para* adduct (**29**) is formed reversibly, readily eliminating the labile chloride ion. The initial *ortho* adduct **30,** however, can readily tautomerize to give the stable aniline derivative **22**−**25**. This mechanism is illustrated in Scheme 4. The lability of the chloride in structure **29** is further established by photolysis of the 4-chloro derivative

Scheme 5. Products from the Chloro/MeOH

Scheme 6. Chloro/Methoxy Mechanism

16 in MeOH (Scheme 5). In this case a mixture of *N*-methyl-4-chloro-2-methoxyaniline **31** and its isomer, *N*-methyl-4-methoxy-2-chloroaniline **24**, is obtained. The latter is the result of initial attack of MeOH on the *para* position, followed by elimination of Cl⁻ and subsequent re-addition of the latter at the *ortho* position, as illustrated in Scheme 6.

3. LFP-TRUV. Pulsed laser (355 nm, 4 mJ, 10 ns) photolysis of the 4-phenyl precursor **15** in CH₃CN gives a short-lived visible absorption band with $\lambda_{max} = 460$ nm, as shown in Figure 1. The species responsible for this band has a lifetime of 24 ± 4 μs in dry CH₃CN.[42] It is assigned to *N*-methyl-*N*-(4-biphenylyl)-nitrenium ion **2** on the basis of the following observations. (1) Addition of the nucleophiles Cl⁻ and MeOH to the LFP samples

(32) Moran, R. J.; Falvey, D. E. *J. Am. Chem. Soc.* **1996**, *118*, 8965−8966.

(33) Srivastava, S.; Kercher, M.; Falvey, D. E. *J. Org. Chem.* **1999**, *64*, 5853−5857.

(34) Takeuchi, H.; Higuchi, D.; Adachi, T. *J. Chem. Soc., Perkin Trans. 2* **1991**, 1525−1529.

(35) Takeuchi, H.; Koyama, K. *J. Chem. Soc., Perkin Trans. 1* **1988**, 2277−2281.

(36) Takeuchi, H.; Hayakawa, S.; Tanahashi, T.; Kobayashi, A.; Adachi, T.; Higuchi, D. *J. Chem. Soc., Perkin Trans. 2* **1991**, 847−855.
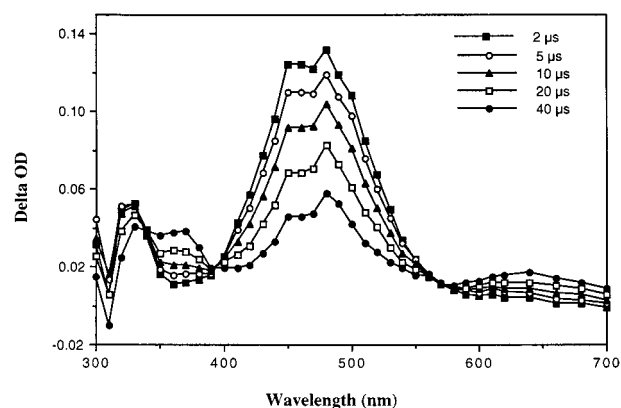
(37) Abramovitch, R. A.; Evertz, K.; Huttner, G.; Gibson, H. H.; Weems, H. G. *J. Chem. Soc., Chem. Commun.* **1988**, 325−327.

(38) Abramovitch, R. A.; Shi, Q. *Heterocycles* **1994**, *37*, 1463−1466.

(39) Takeuchi, H.; Watanabe, K. *J. Phys. Org. Chem.* **1998**, *11*, 478−484.
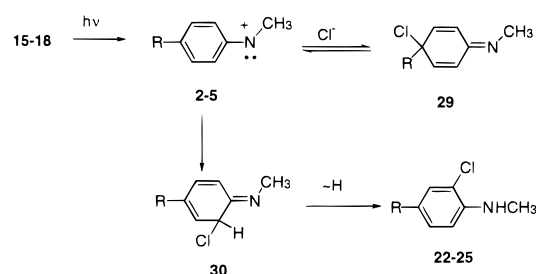
(40) Takeuchi, H.; Hayakawa, S.; Murai, H. *J. Chem. Soc., Chem. Commun.* **1988**, 1287−1289.

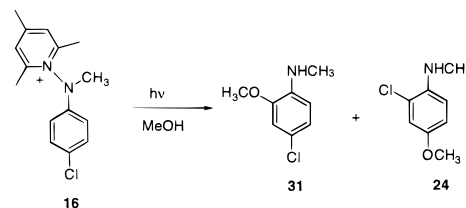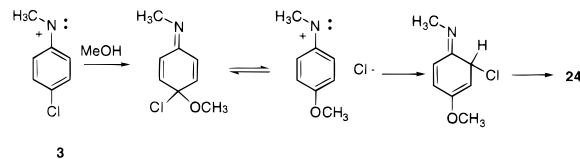(41) Gassman, P. G.; Campbell, G. A. *J. Am. Chem. Soc.* **1972**, *94*, 3891−3896.

(42) Most of the *N*-methyl-*N*-arylnitrenium ions generated in this way decay following first-order kinetics. However, in the absence of trapping agents, the product mixtures are complicated, and the lifetimes probably reflect more than one decay pathway, including hydride shift from the methyl group to the nitrenium center. Chiapperino, D.; Falvey, D. E. *J. Phys. Org. Chem.* **1997**, *10*, 917−924.
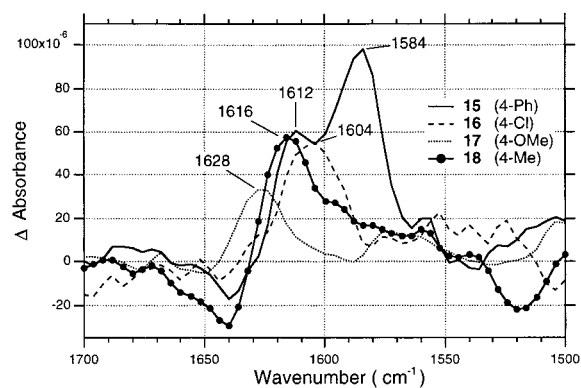
Figure 2. TRIR difference spectra observed over the first 1.0 μs following laser photolysis (266 nm, 10 ns, 0.4 mJ) of pyridinium salts **15−18** in argon-saturated acetonitrile-d_3.

diminishes its lifetime. A pseudo-first-order kinetic analysis provides rate constants of 8×10^9 and 3.7×10^5 M^{-1} s^{-1} for Cl$^-$ and MeOH, respectively. Diffusion-limited reaction with halides and slower reactions with alcohols are characteristic of arylnitrenium ions.[27,29,43] (2) The absorption band is of a similar shape and position to those reported by McClelland et al. for structurally similar 4-biphenylylnitrenium ions.[44−46] (3) Lifetimes measured in O$_2$- and N$_2$-purged solution are indistinguishable. Arylnitrenium ions react slowly, if at all, with O$_2$.

The other derivatives **3−5** were also studied by TRUV. In these cases, lower wavelength excitation (266 or 308 nm) was used to generate the nitrenium ion. The 4-chloro derivative (**3** generated from **16**) absorbs at 340 nm, and its lifetime is 950 ns in CH$_3$CN. This species reacts with Cl$^-$ at the diffusion limit (2.8×10^{10} M^{-1} s^{-1}) and more slowly with MeOH (6.8×10^7 M^{-1} s^{-1}). The 4-methoxy derivative (**4** generated from **17**) absorbs at 320 nm. This spectrum shows good agreement with those reported by McClelland for similar 4-alkoxynitrenium ions.[28,47] In the absence of added traps, nitrenium ion **4** lives for over 100 μs and decays in a kinetically complex manner. When the nucleophilic trap Cl$^-$ is added, the decay is observed to conform to first-order kinetics and a rate constant of 1.7×10^{10} M^{-1} s^{-1} is measured. The 4-methyl derivative (**5** from **18**) shows an absorption maximum at 330 nm and a lifetime of 7.4 μs in CH$_3$CN. It, too is observed to react with Cl$^-$ near the diffusion limit (2.3×10^{10} M^{-1} s^{-1}) and more slowly with MeOH (6.0×10^7 M^{-1} s^{-1}).

4. LFP-TRIR. Figure 2 shows the TRIR difference spectra observed from 1700 to 1500 cm^{-1} over the first 1.0 μs following laser photolysis of the 1-aminopyridinium salts **15−18** in Ar-saturated CD$_3$CN. The negative bands observed near 1640 and 1520 cm^{-1} in Figure 2 are due to the depletion of the pyridinium precursors. The positive bands at 1628−1584 cm^{-1} are assigned to the substituted singlet *N*-methyl-*N*-phenylnitrenium ions **2−5** on the basis of the following. (1) The experimentally observed frequencies are in excellent agreement with the aromatic C=C symmetric stretching frequencies calculated using density functional theory (see below). (2) The observed rate of decay for each of these signals indicates that the lifetimes of **2−5** are

(43) Davidse, P. A.; Kahley, M. J.; McClelland, R. A.; Novak, M. *J. Am. Chem. Soc.* **1994**, *116*, 4513−4514.
(44) McClelland, R. A.; Kahley, M. J.; Davidse, P. A. *J. Phys. Org. Chem.* **1996**, *9*, 355−360.
(45) McClelland, R. A.; Kahley, M. J.; Davidse, P. A.; Hadzialic, G. *J. Am. Chem. Soc.* **1996**, *118*, 4794−4803.
(46) McClelland, R. A.; Davidse, P. A.; Hadzialic, G. *J. Am. Chem. Soc.* **1995**, *117*, 4173−4174.
(47) Ramlall, P.; McClelland, R. A. *J. Chem. Soc., Perkin Trans. 2* **1999**, 225−232.

Table 1. Observed Rates of Decay for 4-Substituted *N*-Methylphenylnitrenium Ions **2−5** in Acetonitrile (TRUV) and in Acetonitrile-d_3 (TRIR)

	k_{obs} (s^{-1})	
	by TRUV	by TRIR
2	4.16×10^4	1.21×10^5
3	1.05×10^6	1.25×10^6
4	$1 \times 10^{4\,a}$	5.98×10^4
5	1.35×10^5	4.92×10^5

[a] Decay does not follow first-order kinetics; the half-life is >100 μs.

Table 2. Electronic State and Zero-Point Vibrational Energies and Singlet−Triplet Splittings for *Para*-Substituted Methylphenylnitrenium Ions[a]

para substituent	electronic state	E	ZPVE (kcal/mol)	S−T splitting[b]
Me	^{1}A′	−365.295 75	0.154 75	−17.0
	^{3}A	−365.266 85	0.152 93	
Cl	^{1}A′	−785.596 96	0.119 34	−17.7
	^{3}A″	−785.568 72	0.117 52	
Ph	^{1}A	−557.041 24	0.207 87	−18.2
	^{3}A	−557.010 20	0.205 86	
MeO	^{1}A′	−440.521 65	0.160 61	−21.3
	^{3}A	−440.485 88	0.158 74	

[a] BPW91/cc-pVDZ level; electronic energies and ZPVE in hartrees, S−T splittings (including ZPVE) in kcal/mol. [b] A negative splitting indicates the singlet state is below the triplet.

consistent with those experimentally determined from TRUV-LFP studies (Table 1). The observed rate constants for nitrenium ion decay were found to increase significantly upon continuous irradiation of the solution, presumably due to trapping of the nitrenium ion by stable products photogenerated during the experiment. One possibility for this trapping agent is 2,4,6-trimethylpyridine, which is expected to trap the nitrenium ions at or near the diffusion limit. Thus, values given in Table 1 represent upper limits for the observed decay rates of **2−5** in argon-saturated acetonitrile-d_3 solutions. The lifetimes follow the expected trend for a series of 4-substituted cations, with the 4-methoxy derivative **4** being the most stable ($\tau = 16.7$ μs) and the 4-chloro-derivative **3** having the shortest lifetime ($\tau = 0.80$ μs). (3) The decay rate constants are unaffected by the presence of O$_2$. (4) The signal for biphenylylnitrenium ion **2** is quenched by nucleophiles such as chloride ion. A pseudo-first-order kinetic analysis using the 1584 cm^{-1} IR band provides a value of 1.4×10^{10} M^{-1} s^{-1} for k_{Cl^-}, in good agreement with the value obtained from TRUV analysis.

5. DFT Calculations. The absolute energies, zero-point energies, and singlet−triplet splittings for the equilibrium geometries of the four *para*-substituted *N*-methyl-*N*-phenylnitrenium ions (**2−5**) are provided in Table 2. Computed harmonic IR frequencies and intensities for two different normal modes in both spin states of the four nitrenium ions are provided in Table 3; the modes are best characterized as the C−N stretching mode and the symmetric combination of the two aromatic (H)C−C(H) stretches (animations of both modes for **2−5** are provided as Supporting Information). The latter mode is computed to be quite intense and corresponds to the mode observed experimentally in the region just above 1600 cm^{-1}. The C−N stretch is computed to be much less intense and is not observed in the experimental spectra—it is discussed below, however, because it provides a different measure of the degree of quinoidal character in the arylnitrenium ion. Yet another measure of quinoidal character is provided by the degree of bond length alternation about the aromatic ring.[5] Heavy atom

Table 3. Selected Harmonic Vibrational Frequencies (cm^{-1}) and Intensities (km/mol) for *Para*-Substituted Methylphenylnitrenium Ions[a]

para substituent	electronic state	frequency (intensity)	
		C−N stretch	sym arom C−C stretch
Me	^{1}A′	1531 (29)	1619 (287) [1616][b]
	^{3}A	1465 (2)	1592 (136)
Cl	^{1}A′	1524 (24)	1604 (269) [1604][b]
	^{3}A″	1465 (0.4)	1575 (96)
Ph	^{1}A	1535 (18)	1619 (183) [1612][b]
			1601 (480) [1584][b,c]
	^{3}A	1446 (76)	1593 (10)
			1596 (305) [c]
MeO	^{1}A′	1550 (9)	1629 (241) [1628][b]
	^{3}A	1460 (7.7)	1607 (90)

[a] BPW91/cc-pVDZ level. [b] Experimental value. [c] Normal mode for the substituent ring.
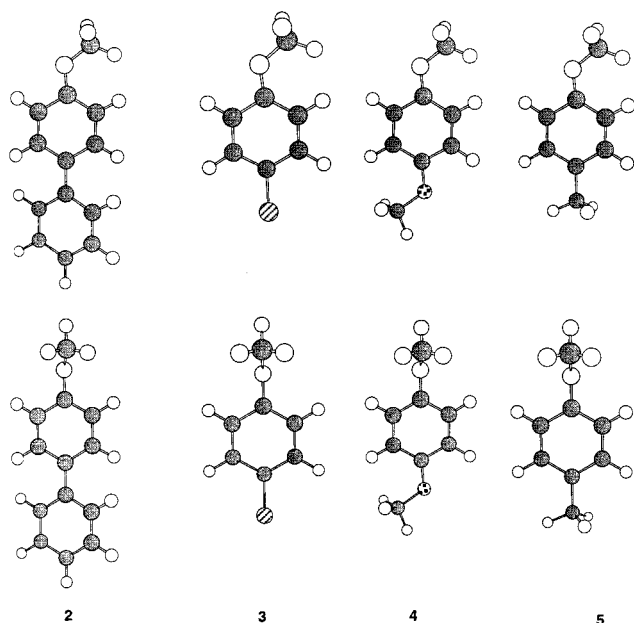
Figure 3. Molecular geometries for *para*-substituted *N*-methyl-*N*-phenylnitrenium ion singlets (above) and triplets (below). Substituents from left to right are *p*-methyl, *p*-chloro, *p*-phenyl, and *p*-methoxy.

bond lengths for both states of the four nitrenium ions are collected in Table 4. Figure 3 illustrates the complete molecular geometries as ball-and-stick models.

Discussion

The formation of nitrenium ions through the photolysis of 1-aminopyridinium ions is well precedented. Takeuchi and Abramovitch first demonstrated this route several years ago.[34−36,38,48] Recently we have used it for LFP investigations of diphenylnitrenium ion and several related species.[33,49,50] The particular 1-aminopyridinium ions studied here follow the expected behavior. Photolysis of **15−18** in the presence of nucleophiles results in the formation of the anticipated ring adducts **22−25**. LFP-TRUV experiments also show typical nitrenium ion UV−vis absorptions. In the case of the 4-phenyl derivative **2** and the 4-methoxy derivative **4**, the TRUV spectra show good agreement with spectra reported by McClelland et

al.[43,47] for similar arylnitrenium ions which lack only the *N*-methyl substituent.

Any remaining doubt that the predicted nitrenium ions are generated is removed by the observation of the characeristic IR bands when photolysis of the same precursors is carried out (Table 1). In the LFP-TRIR experiments, the observed lifetimes are consistently shorter than those measured by LFP-TRUV. This quantitative disagreement is the result of the requirement that the TRIR experiment be conducted at concentrations 20 times higher than those used in the TRUV experiments. We have observed that the lifetime of the nitrenium ion diminishes as the initial concentration of its photoprecursor is increased. In any case, the same general trend is observed with both data sets, where the decay rate constants follow the order **3** > **5** > **2** > **4**.

Arylnitrenium ions have been predicted to possess significant iminocyclohexadienyl cation-like character (Scheme 1).[30] The most obvious manifestation of this comes from the computed C_{ipso}−N bonds lengths ($r8$ in Table 4). For the singlets $r8 = 1.320 \pm 0.003$ Å, placing it much closer to typical values for C=N (1.28 Å) than for C−N (1.40 Å).[51] The data from the 4-substituted phenylnitrenium ions **2−5** allow an examination of electronic factors that influence the structure and reactivity of phenylnitrenium ions. IR spectra (Figure 2) clearly show a shift in the aromatic C=C stretch that is sensitive to substitution in the 4-position. Introduction of electron-donating groups (MeO, Me, Ph) at the 4-position enhances delocalization of the positive charge from the N atom into the ring. This results in the nitrenium ions having more 4-iminocyclohexa-2,5-dienyl cation-like character with a subsequent upward shift in frequency. 4-Chloro-substituted nitrenium ion **3** has an aromatic C=C stretch centered at 1604 cm^{-1}. The presence of this electron-withdrawing group results in a greater localization of the positive charge on the N atom, resulting in an observed aromatic C=C stretch for **3** that is nearly identical with that for 4-chloroaniline.[52]

With respect to theory, the data in Table 2 show the expected qualitative trend in singlet−triplet splittings as a function of *para* substitution, namely that as the π-donating character of the substituent increases, the singlet state is increasingly stabilized over the triplet. A more complete computational study of this phenomenon has been published elsewhere for several 4-substituted-*N*-protiophenylnitrenium ions.[23] For the purposes of this work, which focuses on IR stretching frequencies as reporters of quinoidal character, we simply emphasize that in all four experimentally characterized cases the singlet state is predicted to lie substantially below the triplet. Given that these species were generated by direct photolysis, it is highly unlikely that the observed IR spectra correspond to a triplet transient− this point is also supported by the computed IR frequencies, as will be discussed next.

While analytical computation of the normal modes provides the full $3N − 6$ frequencies expected for nonlinear molecules having N atoms, we focus here on only two modes that are particularly diagnostic of structural differences between the differently substituted nitrenium ions. The C−N stretching frequency is of interest to the extent that it reflects imine character in the nitrenium ion (increasing imine/quinoidal character would be expected to move this stretch to a higher frequency), but the stretch does not appear to be observable in the experimental spectra. This is consistent with the rather low

(48) Abramovitch, R. A.; Beckert, J. M.; Chinnasamy, P.; Xiaohua, H.; Pennington, W.; Sanjivamurthy, A. R. V. *Heterocycles* **1989**, *28*, 623−628.

(49) Moran, R. J.; Cramer, C. J.; Falvey, D. E. *J. Org. Chem.* **1996**, *61*, 3195−3199.

(50) Chiapperino, D.; Anderson, G. B.; Robbins, R. J.; Falvey, D. E. *J. Org. Chem.* **1996**, *61*, 3195−3199.

(51) March, J. *Advanced Organic Chemistry*, 2nd ed.; McGraw-Hill: New York, 1977.

(52) *The Aldrich Library of Infrared Spectra*; Pouchert, C. J., Ed.; Aldrich Chemical Co.: Milwaukee, WI, 1981; p 723.

Table 4. CNC Valence Angle (deg) and Heavy-Atom Bond Lengths (Å) for *Para*-Substituted Methylphenylnitrenium Ions[a]
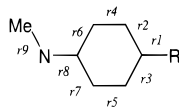
para substituent	electronic state	r1	r2	r3	r4	r5	r6	r7	r8	r9
Me[b]	$^1A'$	1.487	1.440	1.427	1.375	1.380	1.459	1.458	1.323	1.422
	^3A	1.494	1.430	1.426	1.382	1.384	1.445	1.444	1.333	1.413
Cl	$^1A'$	1.705	1.433	1.424	1.376	1.379	1.458	1.458	1.323	1.421
	$^3A''$	1.715	1.422		1.383		1.444		1.334	1.413
Ph	^1A	1.454	1.446	1.438	1.373	1.374	1.458	1.457	1.321	1.428
	^3A	1.461	1.433	1.433	1.382	1.382	1.438	1.438	1.345	1.422
MeO[c]	$^1A'$	1.316	1.445	1.434	1.367	1.373	1.463	1.462	1.317	1.428
	^3A	1.322	1.432	1.427	1.377	1.383	1.442	1.441	1.342	1.419

[a] BPW91/cc-pVDZ level. Bond lengths identical to others by symmetry are not reported. See Figure 3 for ball-and-stick figures. [b] One C−H bond of the substituent methyl group eclipses the C−C bond labeled *r*3 in both states. [c] The O−C bond of the substituent methoxy group eclipses the C−C bond labeled *r*3 in both states.

intensity predicted for this mode by the computations (Table 3). However, a C−C stretching mode in the aromatic ring (symmetric combination of bonds *r*4 and *r*5 as labeled in Table 4) provides a similar measure of quinoidal character, where again the frequency is expected to move to higher frequency with increasing imine character. This absorption is predicted to be much more intense, suggesting that it is, indeed, the mode observed in the experimental spectra.

For the 4-methyl (**5**), -chloro (**3**), and -methoxy (**4**)-substituted cases, we observe nearly quantitative agreement between the experimentally observed IR frequencies in the region just above 1600 cm^{-1} and those computed for the symmetric aromatic stretching mode of the singlet state at the BPW91/cc-pVDZ level. Indeed, the average deviation between theory and experiment is only 1 cm^{-1}! In the *p*-phenyl case (**2**) there are two observed frequencies against which to compare. Agreement between theory and experiment is still very good for the higher frequency mode and somewhat less satisfactory for the lower frequency mode. Nevertheless, the average deviation between theory and experiment over all five observed modes is only 6 cm^{-1}, which is remarkably close agreement.

Comparison of the analogous modes for the triplet states of the four experimentally characterized nitrenium ions gives an average error (unsigned) of 21 cm^{-1}, again suggesting that the observed spectra do not arise from triplet transients. As a last point in this regard, for the biphenylylnitrenium (**2**) triplet it is predicted that the aromatic stretching modes for both rings would overlap in the experimental spectrum. The observed spectrum, however, shows two distinct peaks in this region, with the lower wavelength absorption 18 cm^{-1} below the higher and about twice as intense. This is in excellent agreement with the theoretical predictions for both the separation between the peaks (28 cm^{-1}) and the relative intensities (roughly 2.6:1).

The trend in the IR frequencies is exactly that expected from qualitative considerations. Improved π-donating character of the *para* substituent leads to a shift of the arylnitrenium aromatic stretch absorption to higher frequency. From the chloro to the methoxy substituent, the observed shift is 25 cm^{-1}—theory predicts 24 cm^{-1}. In sum, the agreement between theory and experiment appears to be definitive with respect to the nature and behavior of this normal mode and the assignment of the observed transients to the corresponding nitrenium ion singlet state.

The computations permit an examination of the predicted geometries to assess the degree to which the changes in IR frequencies reflect changes in the relative geometries of the

differently substituted arylnitrenium ions. Bond alternation in a quinoidal sense should give rise to relatively longer bonds *r*2, *r*3, *r*6, and *r*7 and shorter bonds *r*4 and *r*5 (Table 4). In addition, since π-donation is expected to be more stabilizing for the singlet state than for the triplet (since the conjugated nitrogen p orbital is formally empty in the former state but half-filled in the latter), one might expect to see shorter bonds *r*1 and *r*8 in the singlet state than in the triplet state for a given substitution pattern. Finally, since *r*8 and *r*9 are the same kinds of bonds in all four substituted cases, one might predict that increasing quinoidal character with improved π-donation would shorten *r*8 and lengthen *r*9 (since hyperconjugation by the methyl group becomes less important as a stabilizing effect) across the substitution series.

All of these effects are observed in the computed geometries, although they are not as dramatic as those seen in the IR frequencies. In the 4-chloro (**3**) singlet, the average of bond lengths *r*4 and *r*5 is 1.378 Å, and this shortens to 1.370 Å in the 4-methoxy (**4**) singlet. For those respective singlets, the averages for the remaining aromatic bond lengths are 1.443 and 1.451 Å. Thus, the degree of bond alternation (the difference between these two averages) increases with increasing π-donating character of the *para* substituent. This effect does exist in the triplet as well. However, the difference in average bond lengths is reduced in magnitude by about 0.02 Å. The triplets also show longer bonds from the aromatic ring to the substituents (*r*1) and to the nitrenium nitrogen (*r*8), in each case by about 0.01 Å. The latter effect is particularly noteworthy because, in the absence of conjugation effects, bond lengths to triplet nitrenium nitrogen atoms are typically *shorter* than bond lengths to singlet atoms. This is due to the wider bond angle (and hence greater s character in σ bonding orbitals) adopted by the triplet—this hybridization effect *is* observed for *r*9, which is shorter for the triplets than for the singlets by about 0.01 Å.[53,54] With increased π-donation, bond lengths *r*8 and *r*9 do move in the expected directions; from 4-chloro to 4-methoxy, *r*8 decreases by 0.006 Å while *r*9 increases by 0.007 Å.

One final note regarding geometry concerns the rotation about the C$_{ipso}$−N bond in the arylnitrenium ions. In the singlet state, the N−CH$_3$ bond is coplanar with the aromatic system, as

(53) Lim, M. H.; Worthington, S. E.; Dulles, F. E.; Cramer, C. J. In *Density Functional Calculations of Radicals and Diradicals*; Laird, B. B., Ross, R. B., Ziegler, T., Ed.; American Chemical Society: Washington, DC, 1996.

(54) Cramer, C. J.; Dulles, F. J.; Storer, J. W.; Worthington, S. E. *Chem. Phys. Lett.* **1994**, *218*, 387−394.

expected since this maximizes conjugation and allows electron delocalization onto the aggressively π-withdrawing nitrogen atom. In the triplet state, however, the N−CH$_3$ bond is always predicted to be rotated 90° out of the aromatic plane. This presumably relieves some steric congestion associated with the coplanar geometry. In addition, since the triplet nitrenium ions have valence bond angles at nitrogen typically in the range of 130−140°, overlap with the formally sp^2 hybrid at nitrogen is only somewhat reduced compared to the pure p orbital on that atom. As both are half-filled and the former is of lower energy by virtue of its s character, there is not a strong driving force to remain coplanar. This bond rotation is computed to have a very low barrier−coplanar triplets within the systems studied here are typically only 1 or 2 kcal mol^{-1} higher in energy than the equilibrium structures. These results, however, prompted us to reexamine the unsubstituted parent system, *N*-methyl-*N*-phenylnitrenium ion, which was previously predicted by two of us to have a coplanar structure.[16] The coplanar structure, in fact, is a transition state for rotation about the C$_{ipso}$−N bond, but the barrier is a mere 0.02 kcal mol^{-1}; i.e., the situation is that of a free rotor. The observation that singlet and triplet arylnitrenium ions possess very different geometries suggests that it might be possible to engineer a specific system with a long-lived spin isomerism. In such a system the triplet state would be lowest in energy at its equilibrium geometry while the singlet state would be lowest in energy at *its* equilibrium geometry. Berson and co-workers have recently proposed similar long-lived spin isomerism for a substituted non-Kekulé diradical.[55] Likewise, Bally and McMahon have observed a similar spin isomerism for 2-naphthyl(carbomethoxy)carbene. In the latter case the triplet is planar and the singlet is nonplanar.[56]

Conclusions

The excellent quantitative agreement between the theoretically and experimentally derived IR frequencies for singlet nitrenium ions **2**−**5** leads to several important findings. First, it verifies previous conclusions that arylnitrenium ions are the primary products from the photolysis of 1-(*N*-arylamino)pyridinium ions. Second, it demonstrates that the DFT calculations at the levels presented here reliably reproduce key structural features of this family of reactive intermediates. Third, it supports the theoretical prediction that **2**−**5** have singlet ground states. Finally, both the experimental IR frequencies and the DFT calculations indicate that these arylnitrenium ions possess structures that are well described as 4-iminocyclohexa-2,5-dienyl cations.

Experimental and Computational Methods

1-(*N*-(4-Biphenylyl)-*N*-methylamino)-2,4,6-trimethylpyridinium Tetrafluoroborate (15). 1-Methyl-1-(4-biphenylyl)hydazine (**19**, 1.33 g, 7.01 mmol, see Supporting Information for its preparation and characterization) was dissolved in 70 mL of 100% EtOH, and then 1.20 g (5.71 mmol) of freshly prepared 2,4,6-trimethylpyrylium tetrafluoroborate **20**[57] was added to the solution. The reaction mixture was stirred for 30 min, by which time a bright yellow precipitate had formed. The mixture was cooled on an ice bath and then poured into 500 mL of cold diethyl ether to maximize precipitate formation. The product was collected by filtration, and crystals were washed with cold diethyl ether and then dried under reduced pressure. Based on the limiting amount of **20**, a 96% isolated yield (2.14 g, 5.48 mmol) of bright yellow crystals of **15** was obtained: mp 190−192 °C; ^{1}H NMR

(55) Bush, L. C.; Maksimovic, L.; Feng, X. W.; Lu, H. S. M.; Berson, J. A. *J. Am. Chem. Soc.* **1997**, *119*, 1416.

(56) Zhu, Z.; Bally, T.; Stracener, L. L.; McMahon, R. J. *J. Am. Chem. Soc.* **1999**, *121*, 2863−2874.

(57) Balaban, A. T.; Paraschiv, M. *Rev. Roum. Chim.* **1982**, *27*, 513−521.

(400 MHz, CDCl$_3$) δ 7.69 (s, 2 H), 7.56 (d, *J* = 7.7 Hz, 2 H), 7.52 (d, *J* = 8.8 Hz, 2 H), 7.43 (t, *J* = 7.7 Hz, 2 H), 7.33 (t, *J* = 7.7 Hz, 1 H), 6.40 (br d, *J* = 8.8 Hz, 2 H), 3.67 (s, 3 H), 2.67 (s, 3 H), 2.63 (s, 6 H); ^{13}C NMR (100 MHz, CDCl$_3$) δ 161.3, 158.3, 142.9, 139.7, 134.7, 129.7, 129.1, 128.9, 127.2, 126.6, 110.8, 38.4, 22.2, 19.3; MS (FAB) *m/z* (relative intensity) 303 ([M − BF$_4$]$^+$, 46), 182 (100); HRMS (FAB) calcd for C$_{21}$H$_{23}$N$_2$ [M − BF$_4$]$^+$ 303.1861, found 303.1858.

1-(*N*-(4-Chlorophenyl)-*N*-methylamino)-2,4,6-trimethylpyridinium Tetrafluoroborate (16). In a solvent mixture of 15 mL each of water, HOAc, and ethanol stirred on an ice bath, 1.23 g (7.21 mmol) of 4-chloro-*N*-methyl-*N*-nitrosoaniline (**12**, see Supporting Information) was added followed by 4.5 g of finely powdered Zn. After 30 min of stirring, the solution was filtered to remove precipitated salts and then neutralized with aqueous NaHCO$_3$ and solid Na$_2$CO$_3$. The solution was extracted three times with CH$_2$Cl$_2$, the combined organic extracts were dried over MgSO$_4$ and filtered, and the solvent was evaporated under reduced pressure. To this crude product mixture, 10.0 mL of 100% EtOH was added, followed by 0.670 g (3.19 mmol) of freshly prepared **20**. The solution was stirred at room temperature for 40 min, cooled on an ice bath, and added to 200 mL of cold diethyl ether. Light yellow crystals were isolated by filtration, giving 0.930 g (2.66 mmol, 84%) of **16**: mp (EtOH) 178−180 °C; ^{1}H NMR (400 MHz, CDCl$_3$) δ 7.69 (s, 2 H), 7.29 (d, *J* = 8.9 Hz, 2 H), 7.30 (br, 2 H), 3.61 (s, 3 H), 2.65 (s, 3 H), 2.58 (s, 6 H); ^{13}C NMR (100 MHz, CDCl$_3$) δ 161.6, 158.1, 142.3, 130.4, 129.9, 126.9, 111.7, 38.6, 22.2, 19.1; MS (FAB) *m/z* (relative intensity) 261 ([M − BF$_4$]$^+$, 18), 142 (30), 140 (100), 122 (95), 121 (30); HRMS (FAB) calcd for C$_{15}$H$_{18}$ClN [M − BF$_4$]$^+$ 261.11584, found 261.11512.

1-(*N*-(4-Methoxyphenyl)-*N*-methylamino)-2,4,6-trimethylpyridinium Tetrafluoroborate (17). Compound **17** was prepared in the same manner described for the synthesis of **16**. Starting with 1.83 g (11.0 mmol) of nitroso compound **8**, the crude mixture from Zn reduction was combined with 0.840 g (4.00 mmol) of pyrilium salt **20** in EtOH, producing 1.18 g (3.44 mmol) of **17** as a yellow solid, representing an 86% yield: ^{1}H NMR (400 MHz, CDCl$_3$) δ 7.70 (s, 2 H), 6.87 (d, *J* = 9.1 Hz, 2 H), 6.31 (br d, 2 H), 3.75 (s, 3 H), 3.54 (s, 3 H), 2.62 (s, 3 H), 2.58 (s, 6 H); ^{13}C NMR (100 MHz, CDCl$_3$) δ 161.0, 158.3, 154.7, 137.7, 129.8, 115.7, 112.1, 55.7, 38.7, 22.0, 19.2; MS (FAB) *m/z* (relative intensity) 257 ([M + H]$^+$, 11), 136 (100), 122 (34), 121 (14); HRMS (FAB) calcd for C$_{16}$H$_{21}$N$_2$O [M − BF$_4$] 257.1654, found 257.1665.

1-(*N*-Methyl-*N*-4-tolylamino)-2,4,6-trimethylpyridinium Tetrafluoroborate (18). Using the same procedures described above for **16**, 4.40 g of unpurified *N*-methyl-*N*-nitroso-4-toluidine **14** (see Supporting Information) was used in the Zn reduction, along with 2.61 g (12.4 mmol) of pyryllium salt **20**. Filtration to collect the precipitate yielded 4.01 g (12.2 mmol, 98%) of **18** as bright yellow crystals: ^{1}H NMR (400 MHz, CDCl$_3$) δ 7.69 (s, 2 H), 7.12 (d, *J* = 8.5 Hz, 2 H), 6.22 (br d, *J* = 8.5 Hz, 2 H), 3.58 (d, *J* = 1.1 Hz, 3 H), 2.65 (s, 3 H), 2.58 (s, 6 H); ^{13}C NMR (100 MHz, CDCl$_3$) δ 161.1, 158.4, 141.5, 131.2, 131.0, 129.7, 110.5, 38.4, 22.1, 20.3, 19.2; UV−vis (MeCN) 235, 272, 365 nm; MS (FAB) *m/z* (relative intensity) 241 ([M − BF$_4$]$^+$, 72), 122 (64), 121 (19), 120 (100), 91 (15); HRMS (FAB) calcd for C$_{16}$H$_{21}$N$_2$ [M − BF$_4$]$^+$ 241.1705, found 241.1706.

LFP-TRUV. Data from laser flash photolysis with time-resolved ultraviolet−visible absorption detection experiments were collected using either an excimer laser (Questek 2120 with Xe/HCl gas providing 5−12 ns, 308 nm) or a Nd:YAG laser (Continuum Surelite II-10, 4−6 ns, 355 or 266 nm) as the pulsed excitation source. Excitation energies were attenuated such that 5−20 mJ/pulse was used. During a given experiment, the pulse energy varied by approximately 5%. The transient absorptions were monitored using a probe beam from an Oriel 350-W Xe arc lamp passed through the sample cuvette perpendicular to the excitation beam. Transient waveforms were recorded with a LeCroy 9420 digital oscilloscope which digitizes at a rate of 1 point/10 ns with a bandwidth of 350 MHz. Samples for pulsed irradiation were prepared such that the OD of photolabile substrates was approximately 2.0 at the excitation wavelength employed. Minimal sample depletion was confirmed by steady-state UV spectrum measurement after the LFP experiments.

Photoproduct Analysis. Photolyses for GC/MS analysis were carried out on N_2-purged solutions containing 6−11 mg of the stated 1-aminopyridinium salt derivative (**15**−**18**) and 10−15 mM tetra-*n*-butylammonium chloride in 3.0 mL of dry CH_3CN. Photolyses were carried out using the filtered (>295 nm) output from a 300-W Xe arc lamp. Photolysis times ranged from 10 to 20 min. Sample were then directly analyzed by (GC/MS) using an XTI-5 GC column (30 m, 5% phenyl) with a 0.25-mm internal diameter and 0.25-μm film thickness. Argon was used as the mobile phase. The method begins with 4 min at 50 °C, and then the temperature is increased from 50 to 300 °C over 15 min and held at 300 °C for an additional 10 min. Photoproducts **21**−**25** and **31** were identified by comparison of their retention times and EI-MS with those of authentically synthesized compounds (see Supporting Information).

LFP-TRIR. We conducted LFP-TRIR experiments following the method of Hamaguchi and co-workers[58,59] as described previously.[60] Briefly, the broadband output of a $MoSi_2$ IR source (JASCO) is crossed with excitation pulses from a Nd:YAG laser. Changes in IR intensity are monitored by an MCT photovoltaic IR detector (Kolmar Technologies, KMPV11−1-J1), amplified, and digitized with a Tektronix TDS520A oscilloscope. The experiment is conducted in the dispersive mode with a JASCO TRIR-1000 spectrometer. TRIR difference spectra were collected at 16 cm^{-1} resolution using either a Continuum HPO-300 diode-pumped Nd:YAG laser (266 nm, 10 ns, 0.4 mJ) or a Quantronix Q-switched Nd:YAG laser (266 nm, 90 ns, 0.4 mJ) operating at 200 Hz. Kinetic traces were collected using a Continuum Minilite II Nd:YAG laser (266 nm, 5 ns, 1−4 mJ) operating at 20 Hz.

DFT Calculations. All geometries were fully optimized at the density functional (DFT) level using the gradient-corrected functionals of Becke[61] for exchange and of Perdew and Wang[62] for correlation. The cc-pVDZ basis set[63] was used for all calculations. Analytic frequency calculations were carried out at the same level of theory. In addition to providing harmonic frequencies, these calculations were also examined to verify the nature of all stationary points and to calculate zero-point vibrational energies for the singlet−triplet splittings.

Prior studies[16,18,53,54,64−70][64−70] have demonstrated that this level of theory predicts state splittings to within about 2 kcal/mol as compared to either experiment or better-converged quantum mechanical calculations for systems analogous to those studied here. Density functional calculations were carried out using the Gaussian 94 program suite.[71]

Supporting Information Available: Descriptions of the preparation and characterization of synthetic intermediates **7**−**14**, **19**, and **20** as well as photoproducts **22**−**25** and **31** (PDF). This material is available free of charge via the Internet at http://pubs.acs.org. Geometries, energies, and animations of relevant normal modes for **2**−**5** are also available at http://pollux.chem.umn.edu/~sullivan/phNfreq2.

JA001184K

(58) Iwata, K.; Hamaguchi, H. *Appl. Spectrosc.* **1990**, *44*, 1431.

(59) Yuzawa, T.; Kato, C.; George, M. W.; Hamaguchi, H. *Appl. Spectrosc.* **1994**, *48*, 684.

(60) Wang, Y.; Yuzawa, T.; Hamaguchi, H.; Toscano, J. P. *J. Am. Chem. Soc.* **1999**, *121*, 2875.

(61) Becke, A. *J. Chem. Phys.* **1986**, *84*, 4524.

(62) Perdew, J. P.; Burke, K.; Wang, Y. *Phys. Rev. B* **1996**, *54*, 6533.

(63) Dunning, T. H. *J. Chem. Phys.* **1989**, *90*, 1007.

(64) Worthington, S. E.; Cramer, C. J. *J. Phys. Org. Chem.* **1997**, *10*, 755.

(65) Schreiner, P. R.; Karney, W. L.; Schleyer, P. v. R.; Borden, W. T.; Hamilton, T. P.; Schaefer, H. F., III. *J. Org. Chem.* **1996**, *61*, 7030.

(66) Wong, M. W.; Wentrup, C. *J. Org. Chem.* **1996**, *61*, 7022.

(67) Matzinger, S.; Bally, T.; Patterson, E. V.; McMahon, R. J. *J. Am. Chem. Soc.* **1996**, *118*, 1535.

(68) Patterson, E. V.; McMahon, R. J. *J. Org. Chem.* **1997**, *62*, 4398.

(69) Sulzbach, H. M.; Platz, M. S.; Schaefer, H. F., III.; Haddad, C. M. *J. Am. Chem. Soc.* **1997**, *119*, 5682.

(70) Shustov, G. V.; Liu, M. T. H.; Rauk, A. *J. Phys. Chem. A* **1997**, *101*, 2509.

(71) Frisch, M. J.; Trucks, G. W.; Schlegel, H. B.; Gill, P. M. W.; Johnson, B. G.; Robb, M. A.; Cheeseman, J. R.; Keith, T.; Petersson, G. A.; Montgomery, J. A.; Raghavachari, K.; Al-Laham, M. A.; Zakrzewski, V. G.; Ortiz, J. V.; Foresman, J. B.; Cioslowski, J.; Stefanov, B. B.; Nanayakkara, A.; Challacombe, M.; Peng, C. Y.; Ayala, P. Y.; Chen, W.; Wong, M. W.; Andres, J. L.; Replogle, E. S.; Gomperts, R.; Martin, R. L.; Fox, D. J.; Binkley, J. S.; Defrees, D. J.; Baker, J.; Stewart, J. P.; Head-Gordon, M.; Gonzalez, C.; Pople, J. A. *Gaussian 94*, Revision D.1; Gaussian, Inc.: Pittsburgh, PA, 1995.